

Synthesis and X-ray Structures of Elusive Imine/Oxime-Type Organocobalt B₁₂ Complexes. NMR Study Suggesting Steric Strain within the Axially Ligated Benzimidazole

Suzette M. Polson,[†] Renzo Cini,[‡] Claudia Pifferi,[‡] and Luigi G. Marzilli^{*,†}

Department of Chemistry, Emory University, Atlanta, Georgia 30322, and Dipartimento di Scienze e Tecnologie Chimiche e dei Biosistemi, Università di Siena, Pian dei Mantellini 44, 53100 Siena, Italy

Received September 6, 1996[⊗]

Organocobalt B₁₂ model complexes of the imine/oxime-type containing R groups with good *trans* influence were prepared using the isolated Co^I reagent (CO)Co^I((DO)(DOH)pn). Complexes were of the type [LCo((DO)(DOH)pn)R]PF₆ (or ClO₄) (L = H₂O, py, Me₃Bzm for R = CH₂OCH₃; L = H₂O, Me₃Bzm for R = CH₂SCH₃). The –CH₂SCH₃ group is a new ligand for a B₁₂ model system. Different synthetic routes were used to prepare other new complexes of the type [LCo((DO)(DOH)pn)R(or X)]PF₆ (or ClO₄) (L = H₂O, *N*-MeImd, Me₃Bzm for X = Cl; L = py, Me₃Bzm for X = N₃; L = H₂O, py, Me₃Bzm for R = CH₂Cl, CH₂NO₂; L = py for R = CH₂CN). X-ray crystal structures were determined for [Me₃BzmCo((DO)(DOH)pn)CH₂OCH₃]PF₆ (**1**), [pyCo((DO)(DOH)pn)CH₂OCH₃]PF₆ (**2**), and [Me₃BzmCo((DO)(DOH)pn)CH₂Cl]PF₆ (**3**). Combined with previous results, the structures of the new Me₃Bzm complexes create a series of five imine/oxime structures. The trend of axial Co–N bond lengthening with increasing electron-donating ability of the R group found for [Me₃BzmCo((DO)(DOH)pn)R]PF₆ [CH₂CF₃ < CH₂Cl < CH₃ < CH₂CH₃ < CH₂OCH₃] was similar to that of the well-studied cobaloximes LCo(DH)₂R (DH = monoanion of dimethylglyoxime). The axial Co–N and Co–C bonds of the imine/oxime-type complexes were slightly longer compared to the respective bonds in the corresponding cobaloximes. Such a slight dependence of Co–C bond length on the nature of the equatorial ligand has not been established previously. For some carbons, ¹³C NMR chemical shifts for [Me₃BzmCo((DO)(DOH)pn)R(or X)]ClO₄ in CDCl₃ correlated linearly with the electronic parameter (EP), a spectroscopic measure of the electronic *trans* influence. The shifts for [Me₃BzmCo((DO)(DOH)pn)CH₂SCH₃]ClO₄ allowed us to calculate the EP value for the –CH₂SCH₃ group. The value indicates a *trans* influence for –CH₂SCH₃ similar to that of –CH₃. Shifts for some types of carbons in [Me₃BzmCo((DO)(DOH)pn)R(or X)]ClO₄ did not correlate well. This lack of correlation can be attributed, in part, to steric strain in the Me₃Bzm induced by non-bonded repulsions of this axial ligand with the equatorial ligand. The influence of such steric strain is not so evident in the shift trends of the corresponding carbons in cobaloxime analogs. This result suggests less ligand repulsion in the cobaloximes since the orientation of the plane of the Me₃Bzm ligand differs by 60–90° from the analogous plane in the imine/oxime model system.

Introduction

An X-ray crystal structure of the MeB₁₂-binding domain of *Escherichia coli* methionine synthase (MS) revealed that the axial ligand *trans* to the Co–CH₃ bond is not the 5,6-dimethylbenzimidazole (DMBz) attached to the corrin in the cofactor but an imidazole from a histidine residue.¹ Also, there is unambiguous evidence that the DMBz is not bound to Co when coenzyme B₁₂ (AdoB₁₂, 5'-adenosylcobalamin) is bound to methylmalonyl-CoA mutase.^{2,3} These findings have increased the importance of understanding the *trans* influence and *trans* effect in organocobalt chemistry. In particular, the DMBz must dissociate for coenzyme MeB₁₂ to bind to MS. In turn, it is not clear how the new *trans* substituent, i.e. the imidazole from a histidine, influences catalytic turnover. Because the natural B₁₂ cofactors have relatively weakly bound *trans* ligands, organocobalt B₁₂ models containing highly electron-donating negative alkyl axial ligands are of interest for their strong *trans* influence and *trans* effect.⁴

Although negative axial ligands with diverse properties have been readily incorporated into the cobaloxime class of B₁₂ models (LCo(DH)₂R, Chart 1),⁵ a comparable range of axial groups cannot be introduced as easily into other models. Even the closely related imine/oxime-type models {[LCo((DO)(DOH)pn)R]ClO₄ or (PF₆), Chart 1}⁶ pose greater synthetic challenges. We found that carefully controlled conditions in protic solvents allowed us to use the conventional NaBH₄ reduction method to synthesize a more diverse group of alkyl imine/oxime model complexes.⁶ However, some key complexes were unobtainable by this route, even though the analogous cobaloxime complexes could be readily prepared.

B₁₂ model complexes with diverse axial ligands are necessary for elucidating the fundamental relationships among function, structure, and spectra,^{4,7,8} relationships helpful in understanding structural and/or ligating group changes that influence function in B₁₂-dependent processes. The mutual interdependence of the properties of the two *trans* ligands can be assessed by structural,

[†] Emory University.

[‡] Università di Siena.

[⊗] Abstract published in *Advance ACS Abstracts*, January 15, 1997.

- (1) Drennan, C. L.; Huang, S.; Drummond, J. T.; Matthews, R. G.; Ludwig, M. L. *Science (Washington, D.C.)* **1994**, *266*, 1669.
- (2) Mancia, F.; Keep, N. H.; Nakagawa, A.; Leadlay, P. F.; McSweeney, S.; Rasmussen, B.; Bosecke, P.; Diat, O.; Evans, P. R. *Structure* **1996**, *4*, 339.
- (3) Padmakumar, R.; Taoka, S.; Padmakumar, R.; Banerjee, R. *J. Am. Chem. Soc.* **1995**, *117*, 7033.

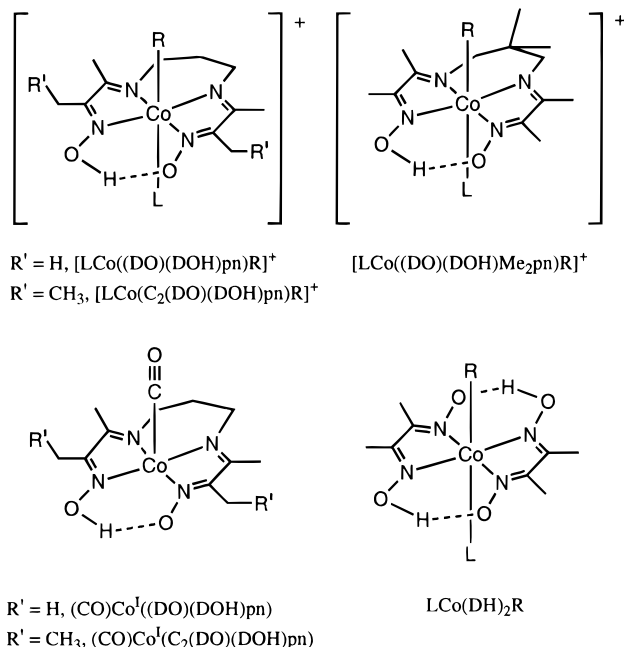
(4) Zangrando, E.; Bresciani-Pahor, N.; Randaccio, L.; Charland, J.-P.; Marzilli, L. G. *Organometallics* **1986**, *5*, 1938.

(5) Bresciani-Pahor, N.; Forcolin, M.; Marzilli, L. G.; Randaccio, L.; Summers, M. F.; Toscano, P. J. *Coord. Chem. Rev.* **1985**, *63*, 1.

(6) Parker, W. O., Jr.; Bresciani-Pahor, N.; Zangrando, E.; Randaccio, L.; Marzilli, L. G. *Inorg. Chem.* **1985**, *24*, 3908.

(7) Marzilli, L. G.; Bayo, F.; Summers, M. F.; Thomas, L. B.; Zangrando, E.; Bresciani-Pahor, N.; Mari, M.; Randaccio, L. *J. Am. Chem. Soc.* **1987**, *109*, 6045.

(8) Charland, J.-P.; Zangrando, E.; Bresciani-Pahor, N.; Randaccio, L.; Marzilli, L. G. *Inorg. Chem.* **1993**, *32*, 4256.

Chart 1. Imine/Oxime and Cobaloxime B₁₂ Model Systems

spectroscopic, thermodynamic, and kinetic methods. Limited comparisons of properties determined by many of these methods suggest that cobalamins and various models have the same type of dependence on the *trans* ligands.⁹ However, anomalies exist; e.g., the ¹³C NMR shifts for only some of the carbons correlate between models and cobalamins.⁹

We are investigating several issues that involve the following: (1) assessing whether the good relationships found for some properties of cobalt corrinoids and a limited set of synthetic B₁₂ compounds are indeed general^{9,10} and not the result of the limited comparisons now possible; and (2) examining if the sources of differences between cobalt corrinoids and models could be understood by correlating the properties of more precisely characterizable model systems with each other.

In this report, we continue our efforts to increase the range of complexes that can be prepared with the imine/oxime-type of cobalt complexes. We compare the properties of these compounds with well-defined, carefully analyzed properties of the cobaloxime model system.^{5,7,8,11} The comparison is intriguing because the closely related compounds differ in many subtle ways. In particular, the orientations of the neutral heterocyclic N-donor ligands differ by 60–90° between the two model systems.

Experimental Section

Preparations. Co((DO)(DOH)pn)Br₂,^{12,13} Co((DO)(DOH)pn)Cl₂,¹³ [pyCo((DO)(DOH)pn)Cl]PF₆,¹⁴ [H₂OCo((DO)(DOH)pn)CH₃]ClO₄,¹⁵ [H₂OCo((DO)(DOH)CH₂Cl)]PF₆,¹⁶ [H₂OCo((DO)(DOH)pn)CH₂CN]-ClO₄,¹⁷ Me₃Bzm = 1,5,6-trimethylbenzimidazole (preparation similar to that for 1-ethyl-5,6-dimethylbenzimidazole),¹⁸ and Me₃BzmCo-

(DH)₂Cl^{8,19} were prepared by previously described methods. [pyCo((DO)(DOH)pn)R]ClO₄ (R = CH₂CF₃, CH₂SCH₃) were generated *in situ* from the aqua analog. For complexes prepared as both ClO₄ and PF₆ salts, only one preparation is described below. These preparations were very similar except usually smaller volumes were used for ClO₄ salts to allow for their greater solubility compared to PF₆ salts. *Caution! Perchlorate salts may be explosive and should be handled in small quantities with appropriate precautions.*²⁰ Dowex 50-X8–100 ion-exchange resin, *N*-MeImd = *N*-methylimidazole, and ClCH₂SCH₃ were from Aldrich. BrCH₂OCH₃ was from Lancaster. Co^I compounds and BrCH₂OCH₃ were stored and dispensed in a drybox under a nitrogen atmosphere. ¹H and ¹³C NMR spectra were recorded on a GE QE-300 MHz NMR spectrometer. All shifts are referenced to TMS (except those of (CO)Co^I((DO)(DOH)pn) which was referenced to CD₃CN at 1.93 ppm). Elemental analyses (Atlantic Microlabs, Atlanta, GA) and additional NMR shifts are tabulated under Results or in the Supporting Information sections.

(CO)Co^I((DO)(DOH)pn). (This is a known compound,²¹ but the synthesis employed was based on the preparation for an analogous compound.²²) To a 500 mL three-necked flask was added a solution of NaOH (1.2 g in 20 mL H₂O) and MeOH (30 mL) and a stir bar, and the level was marked on the flask. Additional MeOH (240 mL) and Co((DO)(DOH)pn)Br₂ (2.36 g, 5.17 mmol) were then added. After 30 min of nitrogen purging, the solution was saturated with carbon monoxide (CP grade) at 0 °C (30 min). A degassed solution of NaBH₄ (0.78 g, 21 mmol in 30 mL H₂O) was then transferred by cannula into the reaction vessel. *Caution! Leave a bleeder needle in the capped NaBH₄ solution to release pressure.* The dark blue solution was stirred and purged with CO for another 15 min, and then MeOH was removed under reduced pressure until the liquid level was just *above* the mark. A dark blue solid was isolated under a nitrogen atmosphere (using a thoroughly purged glovebag), washed with degassed water, and dried under vacuum for several hours. The solid was then transferred in the glovebag to a vial for storage in the drybox. Yield: 1.36 g (81%). ¹H NMR (CD₃CN): δ 1.89 (s, 6H), 2.01 (s, 6H), 2.12 (m, 1H), 2.43 (m, 1H), 3.41 (m, 2H), 3.70 (m, 2H), 19.30 (s, 1H).

[H₂OCo((DO)(DOH)pn)CH₂OCH₃]PF₆. This compound was prepared from the intermediate BrCo((DO)(DOH)pn)CH₂OCH₃. In the drybox, a green-blue THF solution of (CO)Co^I((DO)(DOH)pn) (0.40 g, 1.2 mmol in 40 mL) was treated with CH₃OCH₂Br (0.10 mL, 1.2 mmol). After 1.5 h of rapid stirring, the solution turned orange-brown. The orange solid that precipitated after 2 days was isolated, washed quickly with Et₂O, and vacuum-dried. The air-stable but crude product was dissolved in MeOH and filtered through a fine frit to remove undissolved impurities, and the solvent was removed. This intermediate, BrCo((DO)(DOH)pn)CH₂OCH₃ (0.15 g, 1.2 mmol), was dissolved in a 1:1 MeOH:H₂O mixture (24 mL). A solution of KPF₆ (1.11 g in 40 mL of H₂O) was added, followed by AgNO₃ (0.20 g, 1.2 mmol). After the mixture was stirred for 30 min, AgBr was removed by filtration through Celite. The solution was concentrated to 20 mL, and a red precipitate formed. The solid was collected and washed with Et₂O. Yield: 0.50 g (82%).

[pyCo((DO)(DOH)pn)CH₂OCH₃]PF₆. Py (0.052 mL, 0.64 mmol) was added to a methanolic solution of [H₂OCo((DO)(DOH)pn)CH₂OCH₃]PF₆ (0.30 g, 0.59 mmol, in 40 mL). After the solution was stirred overnight, the MeOH was removed by rotary evaporation, and excess py was removed from the oil by extraction with Et₂O. After 4 h under vacuum, the oil hardened to an orange solid, which was collected and washed with water and Et₂O. Yield: 0.17 g (51%). This solid was recrystallized as orange prisms from acetone/H₂O.

[Me₃BzmCo((DO)(DOH)pn)CH₂OCH₃]PF₆. A solution of [H₂OCo((DO)(DOH)pn)CH₂OCH₃]PF₆ (0.10 g, 0.20 mmol, in 15 mL

- (9) Calafat, A. M.; Marzilli, L. G. *J. Am. Chem. Soc.* **1993**, *115*, 9182.
 (10) Gerli, A.; Sabat, M.; Marzilli, L. G. *J. Am. Chem. Soc.* **1992**, *114*, 6711.
 (11) Randaccio, L.; Geremia, S.; Zangrando, E.; Ebert, C. *Inorg. Chem.* **1994**, *33*, 4641.
 (12) Parker, W. O., Jr. Ph.D. Thesis, Emory University, 1987.
 (13) Costa, G.; Mestroni, G.; de Savognani, E. *Inorg. Chim. Acta* **1969**, *3*, 323.
 (14) Gerli, A.; Marzilli, L. G. *Inorg. Chem.* **1992**, *31*, 1152.
 (15) Parker, W. O., Jr.; Zangrando, E.; Bresciani-Pahor, N.; Randaccio, L.; Marzilli, L. G. *Inorg. Chem.* **1986**, *25*, 3489.
 (16) Polson, S. M.; Hansen, L.; Marzilli, L. G. *J. Am. Chem. Soc.* **1996**, *118*, 4804.

- (17) Parker, W. O., Jr.; Zangrando, E.; Bresciani-Pahor, N.; Marzilli, P. A.; Randaccio, L.; Marzilli, L. G. *Inorg. Chem.* **1988**, *27*, 2170.
 (18) Simonav, A. M.; Pozharskii, A. E.; Marianovskii, V. M. *Ind. J. Chem.* **1967**, *5*, 81.
 (19) Trogler, W. C.; Stewart, R. C.; Epps, L. A.; Marzilli, L. G. *Inorg. Chem.* **1974**, *13*, 1564.
 (20) Raymond, K. N. *Chem. Eng. News* **1983**, *61* (Dec 5), 4.
 (21) Costa, G.; Mestroni, G.; Tazher, G. *J. Chem. Soc., Dalton Trans.* **1972**, 450.
 (22) Finke, R. G.; Smith, B. L.; McKenna, W. A.; Christian, P. A. *Inorg. Chem.* **1981**, *20*, 687.

of MeOH) was treated with Me₃Bzm (0.035 g, 0.22 mmol, in 3 mL of MeOH). After the solution was stirred overnight, MeOH was removed by rotary evaporation. The residue was dissolved in CH₂Cl₂, the solution was filtered through a cotton-plugged pipet, and Et₂O was added. The dark red solid that formed from the chilled (5 °C) mixture was isolated and washed with Et₂O. Yield: 0.092 g (72%). This solid was recrystallized from acetone/H₂O.

[H₂OCo((DO)(DOH)pn)CH₂SCH₃]PF₆. In the drybox, a green-blue solution of (CO)Co^I((DO)(DOH)pn) (0.20 g, 0.61 mmol in 40 mL of THF) was treated with ClCH₂SCH₃ (0.051 mL, 0.61 mmol). After the green solution was stirred for 2 days, the solvent was removed under aerobic conditions (the color changed to brown). The residue was dissolved in MeOH, and the solution was filtered through a fine frit (removing a green solid). MeOH was removed from the filtrate, and the residue was dissolved in 60% MeOH/H₂O (10 mL). AgNO₃ (0.10 g, 0.061 mmol) was added, and the mixture was stirred for 30 min before AgCl was removed by filtration (through Celite), leaving a clear red solution. An aqueous solution of KPF₆ was added (0.56 g, 3.0 mmol). Removal of the MeOH precipitated a gooey solid. The rest of the solvent was then removed. The residue was redissolved in MeOH and the solution filtered to remove the excess of KPF₆. MeOH was removed by rotary evaporation, and the resulting rust-colored solid was dried under vacuum. Yield: 0.17 g (53%).

[Me₃BzmCo((DO)(DOH)pn)CH₂SCH₃]PF₆. A solution of [H₂OCo((DO)(DOH)pn)CH₂SCH₃]PF₆ (0.053 g, 0.10 mmol, in 10 mL of MeOH) was treated with Me₃Bzm (0.018 g, 0.11 mmol, in 1 mL of MeOH), and the mixture was stirred overnight. MeOH was removed, the residue was converted to a dark orange solid, and excess Me₃Bzm was removed by trituration with Et₂O. This trituration was repeated several times, and between each, the residue was dissolved in CH₂Cl₂ and the solvent removed. Yield: 0.039 g (59%).

[Me₃BzmCo((DO)(DOH)pn)Cl]ClO₄. Me₃Bzm (0.23 g, 1.4 mmol) was added to a suspension of Co((DO)(DOH)pn)Cl₂ (0.52 g, 1.4 mmol) in 50% aqueous methanol (50 mL). The red solution was filtered after 30 min of stirring. The filtrate was treated with NaClO₄ (1.0 g, 7.1 mmol), and a fine pink solid precipitated within 1 min. The solid was isolated, washed with H₂O and MeOH (turned brown), and vacuum-dried. Yield: 0.59 g (71%).

[N-MeImdCo((DO)(DOH)pn)Cl]ClO₄. N-MeImd (0.216 mL, 2.71 mmol) was added to a suspension of Co((DO)(DOH)pn)Cl₂ (1.00 g, 2.71 mmol) in 50% aqueous methanol (75 mL). After the solution was filtered, a solution of NaClO₄ (1.2 g in 20 mL H₂O) was added, and a fine pink solid precipitated within 1 min. The solid was isolated, washed with H₂O, and vacuum-dried. Yield: 0.89 g (64%). ¹H NMR (DMSO-*d*₆): δ 1.86 (m, 1H), 2.42 (m, 1H), 2.52 (s, 6H), 2.68 (s, 6H), 3.60 (s, 3H), 4.04 (m, 4H), 6.28 (s, 1H), 7.22 (s, 1H), 7.27 (s, 1H), 18.89 (s, 1H).

[pyCo((DO)(DOH)pn)N₃]PF₆. A solution of [pyCo((DO)(DOH)pn)Cl]PF₆ (0.25 g, 0.45 mmol) in a 2:1 MeOH:H₂O mixture (75 mL) was treated with NaN₃ (0.029 g, 0.45 mmol, in 1 mL of H₂O). Dark red needles formed after slow evaporation (overnight) of MeOH in the hood. The needles were collected, washed with H₂O and Et₂O, and vacuum-dried. Subsequent fractions were collected as more MeOH evaporated. Yield: 0.13 g (44%). ¹H NMR (acetone-*d*₆): δ 2.28 (m, 2H), 2.62 (s, 6H), 2.83 (s, 6H), 4.32 (m, 4H), 7.48 (t, 2H), 8.00 (m, 3H), 18.81 (s, 1H).

[Me₃BzmCo((DO)(DOH)pn)N₃]ClO₄. A light brown suspension of [Me₃BzmCo((DO)(DOH)pn)Cl]ClO₄ (0.097 g, 0.16 mmol) in a 2:1 MeOH:H₂O mixture (15 mL) was treated with NaN₃ (0.011 g, 0.16 mmol). The color changed to red. After the solution was stirred overnight, a fine light brown solid precipitated. The solid was collected, washed with H₂O, and dried under vacuum. Yield: 0.048 g (50%).

Me₃BzmCo(DH)₂N₃. A suspension of Me₃BzmCo(DH)₂Cl (0.22 g, 0.45 mmol) in a 2:1 acetone:H₂O mixture (60 mL) was treated with NaN₃ (0.12 g, 1.8 mmol). The red solution was stirred overnight. The volume was reduced by half, and a fine tan solid precipitated. The solid was collected on a fine frit, washed with H₂O, and vacuum-dried. Yield: 0.10 g (45%). ¹H NMR (CDCl₃): δ 2.34 (s, 3H), 2.37 (s, 12H), 2.38 (s, 3H), 3.75 (s, 3H), 7.04 (s, 1H), 7.85 (s, 1H), 7.96 (s, 1H).

[H₂OCo((DO)(DOH)pn)CH₂NO₂]ClO₄. This compound was prepared from the intermediate complex [N-MeImdCo((DO)(DOH)pn)-

CH₂NO₂]ClO₄ by a modification of the synthesis for pyCo(DH)₂CH₂NO₂.²³ A solution of [N-MeImdCo((DO)(DOH)pn)Cl]ClO₄ (1.67 g, 3.24 mmol) in nitromethane (26 mL) was heated to a constant temperature of ~55 °C, and Ag₂O (0.75 g, 3.25 mmol) was added. The hot mixture was passed through Celite after 1.5 h of stirring, and the filtrate was allowed to stand overnight. The excess of nitromethane was removed by rotary evaporation, and CH₂Cl₂ (100 mL) was added. The insoluble yellow powder, [N-MeImdCo((DO)(DOH)pn)CH₂NO₂]ClO₄, was isolated by filtration. Yield: 1.09 g (62%). A solution of this N-MeImd adduct (1.09 g, 2.02 mmol) in acetone (100 mL), MeOH (50 mL), and water (10 mL) was treated with Dowex 50-X8-100 ion-exchange resin (1.56 g), and the mixture was stirred at ~40 °C for 3.5 h. The resin was removed by filtration, and the solvent was then removed by rotary evaporation. The residue was washed with cold H₂O and dried under vacuum to give a dark orange powder. Yield: 0.34 g (35%).

[pyCo((DO)(DOH)pn)CH₂NO₂]ClO₄. A suspension of [H₂OCo((DO)(DOH)pn)CH₂NO₂]ClO₄ (0.10 g, 0.21 mmol) in acetone (15 mL) was treated with py (0.019 mL, 0.23 mmol), and the solution was stirred overnight. The dark orange mixture was filtered, and the solvent was removed by rotary evaporation. Excess py was removed by trituration with Et₂O, yielding an orange solid. Before each treatment with Et₂O, the residue was dissolved in CH₂Cl₂, and the solvent was removed. Yield: 0.093 g (82%).

[Me₃BzmCo((DO)(DOH)pn)CH₂NO₂]ClO₄. A suspension of [H₂OCo((DO)(DOH)pn)CH₂NO₂]ClO₄ (0.10 g, 0.21 mmol) in acetone (15 mL) was treated with a solution of Me₃Bzm (0.037 g, 0.23 mmol in 1 mL of MeOH). The solution, which turned orange after several hours of stirring, was filtered and the solvent removed. Excess Me₃Bzm was removed from the residue by extraction with Et₂O to give an orange solid. Yield: 0.093 g (72%).

[pyCo((DO)(DOH)pn)CH₂CN]PF₆. A suspension of [H₂OCo((DO)(DOH)pn)-CH₂CN]PF₆ (0.075 g, 0.16 mmol) in acetone (25 mL) was treated with py (0.036 mL, 0.44 mmol). After the mixture was stirred overnight, it was filtered through a fine frit to remove undissolved material. An aqueous solution of KPF₆ (0.14 g) was added to the filtrate, and acetone was removed by rotary evaporation until precipitation occurred. The yellow solid was collected, washed with Et₂O, and dried under vacuum. Yield: 0.020 g (33%).

[Me₃BzmCo((DO)(DOH)pn)CH₂Cl]PF₆·0.8CH₂Cl₂. [H₂OCo((DO)(DOH)pn)CH₂Cl]PF₆ (0.24 g, 0.47 mmol) was dissolved in MeOH (20 mL), and a solution of Me₃Bzm (0.094 g, 0.59 mmol) in MeOH (2 mL) was added. After the orange solution was stirred overnight, a fine yellow powder precipitated. The solid was collected on a fine frit and washed with Et₂O. Yield: 0.17 g (53%). This compound was recrystallized from CH₂Cl₂/Et₂O.

[pyCo((DO)(DOH)pn)CH₂Cl]PF₆. [H₂OCo((DO)(DOH)pn)-CH₂Cl]PF₆ (0.15 g, 0.29 mmol) was suspended in CH₂Cl₂ (20 mL), and py (0.12 mL, 1.47 mmol) was added. The solution was stirred overnight and filtered, and the solvent was removed under reduced pressure. Et₂O was added to a concentrated CH₂Cl₂ solution of the residue until it became cloudy. Orange needles were collected from the cooled mixture and washed with Et₂O. Yield: 0.035 g (19%).

X-ray Crystallographic Data. [Me₃BzmCo((DO)(DOH)pn)-CH₂OCH₃]PF₆ (**1**) and [pyCo((DO)(DOH)pn)CH₂OCH₃]PF₆ (**2**) were recrystallized from acetone/H₂O. Single crystals of [Me₃BzmCo((DO)(DOH)pn)CH₂Cl]PF₆ (**3**) were grown from CH₂Cl₂/Et₂O. A red-orange crystal of **1** (0.30 × 0.40 × 0.40 mm), an orange crystal of **2** (0.30 × 0.40 × 0.60 mm), and a red-orange crystal of **3** (as the CH₂Cl₂ solvate, 0.25 × 0.45 × 0.45 mm) were each mounted on a glass fiber and used for data collection on an Enraf Nonius CAD4 (**1**) or on a Siemens P4 (**2**, **3**) diffractometer. Cell parameters and orientation matrices were calculated from least-squares refinement of the angles of 25 randomly selected reflections (10 < 2θ < 30° (**1**) and 10 < 2θ < 40° (**2**, **3**)). Three standard reflections were measured every 2 h; there was no significant decrease in the intensities. Data were corrected for Lorentz-polarization effects and for absorption through the ψ-scan technique. Detailed crystallographic data are presented in Table 1.

Table 1. Crystallographic Data for [Me₃BzmCo((DO)(DOH)pn)CH₂OCH₃]PF₆ (**1**), [py(Co((DO)(DOH)pn)CH₂OCH₃)]PF₆ (**2**), and [Me₃BzmCo((DO)(DOH)pn)CH₂Cl]PF₆ (**3**)

	1	2	3
empirical formula	C ₂₃ H ₃₆ CoN ₆ F ₆ O ₃ P	C ₁₈ H ₂₉ CoN ₅ F ₆ O ₃ P	C ₂₂ H ₃₃ ClCoF ₆ N ₆ O ₂ P·CH ₂ Cl ₂
fw	648.5	567.4	737.83
temp, K	295 ± 2	295 ± 2	293 ± 2
wavelength, Å	0.710 73	0.710 73	0.710 73
space group	P2 ₁ /c (No. 14)	Cc (No. 9)	P2/c (No. 13)
a, Å	7.490(2)	12.231(2)	17.467(2)
b, Å	22.077(2)	11.659(2)	7.906(2)
c, Å	17.894(2)	17.810(3)	23.351(3)
β, deg	93.38(2)	106.70(2)	102.870(10)
V, Å ³	2954(1)	2432.6(5)	3143.6(10)
Z	4	4	4
ρ _{calc} , g·cm ⁻³	1.458	1.549	1.559
abs coeff, cm ⁻¹	7.03	8.41	9.20
R ₁ ^a	0.0592	0.0337	0.0496
R _w ^b	0.0631	0.0357	
wR ₂ ^c			0.1144
w = a/(σ _F ² + bF ²)	a = 5.540 00 b = 0.000 14	a = 1.000 00 b = 0.002 73	
w = 1/[σ _F ² + (qP) ² + rP]			P = (Max(F _o ²) + 2F _c ²)/3 q = 0.0643 r = 3.15

$$^a \sum |F_o - |F_c|| / \sum F_o, \quad ^b \sum (w|F_o - |F_c|| / \sum wF_o)^{1/2}, \quad ^c [\sum w(F_o^2 - F_c^2)^2 / \sum w(F_o^2)^2]^{1/2}.$$

Solution and Refinement of Structures. The structures were solved through the Patterson and Fourier synthesis techniques and refined via full-matrix least-squares cycles. Attempts at structure solution of **2** in the C2/c space group were not successful. Scattering factors for neutral atoms of **1** and **2** were from SHELX-86,²⁴ SHELX-76,²⁵ SHELX-93 (refinement of the structure of **3**),²⁶ and ref 27. All the calculations were carried out through the SHELX-86 (solution of structures),²⁴ SHELX-76 (refinement of the structures of **1** and **2**),²⁵ SHELX-93 (refinement of the structure of **3**),²⁶ and PARST-95 (analysis of the molecular geometries)²⁸ packages. The Co, P, F, O, N, and C atoms were refined anisotropically,²⁹ whereas the H atoms were treated isotropically. The hydrogen atom of the oxime bridge and those linked to the aromatic ring were located from the Fourier difference maps. The other hydrogen atoms were set in calculated positions and allowed to ride on the atoms to which they are linked.

The weighted agreement index for **2** increased significantly (from 0.0357 to 0.0397) when the sign of all the coordinates was changed. The Flack parameter for the present set of coordinates is 0.0022 (0.0171). These results show that the coordinate set used (see Supporting Information) was correct.

Two crystallographically independent CH₂Cl₂ molecules at 0.5 occupancy each were located in the lattice of **3** through the Fourier synthesis. The C atom of one of the CH₂Cl₂ molecules is sitting on a mirror plane, and the relevant Cl atoms are affected by a statistical disorder. The second CH₂Cl₂ molecule is close to a crystallographic 2-fold axis. Disorder also affects the PF₆⁻ ion; the occupancies of the two sets of six F atoms were fixed at 0.8 and 0.2, respectively.

Results and Discussion

Synthetic Methods. We are exploring the reasons for the difficulty in extending the straightforward synthetic chemistry of cobaloximes to the relatively similar imine/oxime models. Previously, we found that complexes with bulky R groups

containing electron-withdrawing substituents could not be prepared from Co(DO)(DOH)pn)Br₂, using the NaBH₄ reduction method, although analogous preparations worked well with cobaloxime precursors. The suspected problem was product reduction by excess NaBH₄. Controlled-potential electrolysis showed promise for circumventing this problem for imine/oxime models.³⁰ In addition, while methoxide acts as a nucleophile converting LCo(DH)₂CH₂Br complexes to the -CH₂OCH₃ complex,⁴ it deprotonates the Schiff base methyl groups of [LCo((DO)(DOH)pn)CH₂Br]⁺ complexes to produce an enamine anion, which closes to a rare three-membered Co-C-N metallacycle.¹⁶ Such a facile competing ring-closure reaction is not possible for cobaloximes. Thus, some of the reasons that more diverse cobaloximes can be prepared are clear.

In this study, we used (CO)Co^I((DO)(DOH)pn) to prepare complexes containing R groups having a strong *trans* influence. Our synthesis of (CO)Co^I((DO)(DOH)pn) was based on a modification of the method already known for the imine/oxime-type Co^I compound (CO)Co^I(C₂(DO)(DOH)pn) (Chart 1).²² The reported synthesis of (CO)Co^I(C₂(DO)(DOH)pn) involves first preparing Co(C₂(DO)(DOH)pn)₂, which requires two purification steps (53% yield).²² Our method uses Co((DO)(DOH)pn)Br₂, which requires no purification (~50% yield). We also found that the double Schlenk apparatus used for the reduction of Co(C₂(DO)(DOH)pn)₂ to Co^I can be replaced by a three-necked flask and that the time-consuming freeze-pump-thaw cycles for solvent pretreatment can be eliminated, with no sacrifice in yield of Co^I(CO) product (70–80% in both cases). (CO)Co^I(C₂(DO)(DOH)pn) was difficult to obtain analytically pure, but the compound was reported to be sufficiently pure for the synthesis of well-characterized organocobalt products.²² In contrast, we obtained a satisfactory elemental analysis (C,H,N) for (CO)Co^I((DO)(DOH)pn) using our modification of the method.

It is worth comparing the Co^I(CO) method to the widely used NaBH₄ method. While the use of the Co^I(CO) synthesis introduces an isolation step, the alkylation step requires only solvent and one other reagent, the organic halide (RX). An isolated Co^I complex was found to be particularly useful when

(24) Sheldrick, G. M. SHELX-86: Program for the solution of crystal structures. University of Göttingen, Germany, 1986.

(25) Sheldrick, G. M. SHELX-76: Program for the solution of crystal structures. Cambridge University, U.K., 1976.

(26) Sheldrick, G. M. SHELX-93: Program for the refinement of crystal structures. University of Göttingen, Germany, 1993.

(27) *International Tables for X-ray Crystallography*; Kynoch: Birmingham, England, 1974; Vol. IV.

(28) Nardelli, M. PARST: A System of Computer Routines for Calculating Molecular Parameters from Results of Crystal Structure Analyses. *Comput. Chem.* **1983**, *7*, 95.

(29) For **3**, the F(7), F(8), F(9), F(10), F(11), and F(12) atoms were refined isotropically.

(30) Seeber, R.; Parker, W. O., Jr.; Marzilli, P. A.; Marzilli, L. G. *Organometallics* **1989**, *8*, 2377.

oxidative addition of RX required a longer reaction time, an aprotic solvent, and/or a higher reaction temperature.

The $\text{Co}^{\text{I}}(\text{CO})$ method allowed us to prepare the $-\text{CH}_2\text{OCH}_3$ and the $-\text{CH}_2\text{SCH}_3$ imine/oxime complexes, which cannot be prepared by the conventional NaBH_4 route. The $-\text{CH}_2\text{SCH}_3$ complex is not known for the cobaloximes or other B_{12} model systems. Previously, using the NaBH_4 route, we were able to prepare only $\text{R} = \text{CH}_3$ derivatives of the type $[\text{LCo}(\text{DO})(\text{DOH})\text{Me}_2\text{pn}]\text{R}]\text{PF}_6$ (Chart 1).³¹ This equatorial ligand has properties similar to those of $(\text{DO})(\text{DOH})\text{pn}$, but it is bulkier.³¹ We have successfully used the $\text{Co}^{\text{I}}(\text{CO})$ method to prepare $(\text{DO})(\text{DOH})\text{Me}_2\text{pn}$ complexes with several moderately bulky alkyl groups but not with the moderately bulky $-\text{CH}_2\text{OCH}_3$ group.³² The $\text{Co}^{\text{I}}(\text{CO})$ method also failed when we applied it to the synthesis of $[\text{H}_2\text{OC}(\text{DO})(\text{DOH})\text{pn}-i\text{-C}_3\text{H}_7]\text{PF}_6$, although this complex can be obtained by the conventional NaBH_4 route.⁶ These limitations of the $\text{Co}^{\text{I}}(\text{CO})$ method suggest that a combination of steric and electronic effects may be responsible for the lower reactivity, consistent with the suggestion that CO renders Co^{I} compounds less reactive toward oxidative addition.²²

We synthesized the chloro complexes $[\text{Me}_3\text{BzmCo}(\text{DO})(\text{DOH})\text{pn}]\text{Cl}]\text{ClO}_4$ and $[\text{N-MeImdCo}(\text{DO})(\text{DOH})\text{pn}]\text{Cl}]\text{ClO}_4$ by adapting the method known for $[\text{pyCo}(\text{DO})(\text{DOH})\text{pn}]\text{Cl}]\text{PF}_6$.¹⁴ Chloro complexes are useful for obtaining insight into B_{12} model properties because the chloro ligand has a very weak *trans* influence. In addition, these complexes serve as precursors for a number of other new compounds with weak *trans* influence ligands. $[\text{Me}_3\text{BzmCo}(\text{DO})(\text{DOH})\text{pn}]\text{Cl}]\text{ClO}_4$ and $[\text{pyCo}(\text{DO})(\text{DOH})\text{pn}]\text{Cl}]\text{ClO}_4$ were used to prepare the azido analogs $[\text{LCo}(\text{DO})(\text{DOH})\text{pn}]\text{N}_3]\text{ClO}_4$ (or PF_6) ($\text{L} = \text{Me}_3\text{Bzm}$, py), by treatment with NaN_3 . $[\text{N-MeImdCo}(\text{DO})(\text{DOH})\text{pn}]\text{Cl}]\text{ClO}_4$ was converted by known procedures^{17,23} to $[\text{H}_2\text{OC}(\text{DO})(\text{DOH})\text{pn}]\text{CH}_2\text{NO}_2]\text{ClO}_4$. $[\text{LCo}(\text{DO})(\text{DOH})\text{pn}]\text{CH}_2\text{NO}_2]\text{ClO}_4$ ($\text{L} = \text{Me}_3\text{Bzm}$, py) were then prepared by treatment of the aqua analog with L . Our attempts to prepare $[\text{pyCo}(\text{DO})(\text{DOH})\text{pn}]\text{CH}_2\text{NO}_2]\text{ClO}_4$ directly from the chloro derivative were unsuccessful because of py loss under the synthetic conditions.

The new imine/oxime-type complexes containing R groups with either poor or strong *trans* influence allowed us to assess the *trans* influence in this series by both X-ray crystallography and NMR spectroscopy. The PF_6 salts proved useful for characterization by X-ray methods. The high solubility of $[\text{Me}_3\text{BzmCo}(\text{DO})(\text{DOH})\text{pn}]\text{R}]\text{ClO}_4$ complexes in CDCl_3 made these salts most useful for investigating NMR trends. When the axial R or X ligand had a weak *trans* influence, solubility problems were encountered frequently when $\text{L} = \text{py}$ or when the counterion was PF_6^- .

Structural Studies. There are only about one-sixth as many imine/oxime models characterized structurally by X-ray crystallography as cobaloximes.^{5,33} Since in half of the imine/oxime-type structures R is CH_3 ,^{6,15,17,31,34–38} there is not sufficient information for comprehensive structural comparisons between imine/oxime and cobaloxime complexes. However, with the

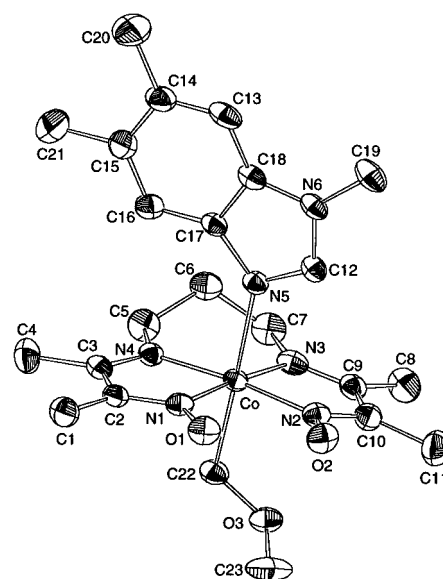


Figure 1. Perspective drawing of the complex molecule of **1** with the atom labels. Ellipsoids enclose 30% probability.

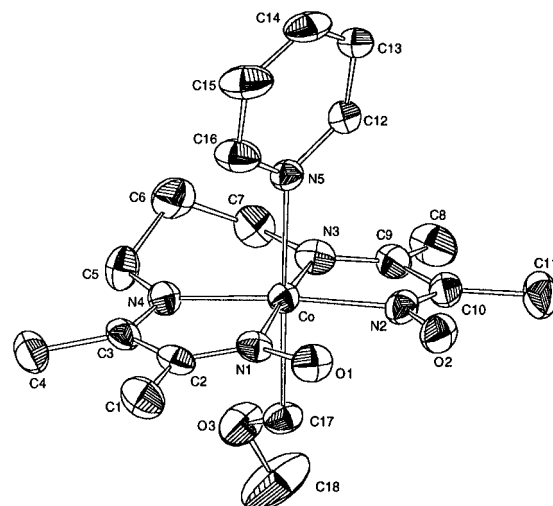


Figure 2. Perspective drawing of the complex molecule of **2** with the atom labels. Ellipsoids enclose 30% probability.

new results, a series of five $[\text{Me}_3\text{BzmCo}(\text{DO})(\text{DOH})\text{pn}]\text{R}]\text{PF}_6$ structures spanning a significant *trans* influence range ($\text{R} = \text{CH}_2\text{CF}_3$, CH_2Cl , CH_3 , CH_2CH_3 , CH_2OCH_3) is available. The new information allows some new distinctions to be drawn between imine/oxime species and cobaloximes.

Perspective drawings of $[\text{Me}_3\text{BzmCo}(\text{DO})(\text{DOH})\text{pn}]\text{CH}_2\text{OCH}_3]\text{PF}_6$ (**1**), $[\text{pyCo}(\text{DO})(\text{DOH})\text{pn}]\text{CH}_2\text{OCH}_3]\text{PF}_6$ (**2**), and $[\text{Me}_3\text{BzmCo}(\text{DO})(\text{DOH})\text{pn}]\text{CH}_2\text{Cl}]\text{PF}_6$ (**3**) are given in Figures 1–3, respectively. Selected bond lengths and angles for these complexes are given in the Supporting Information.

The orientation of the L plane can be described by the torsion angle ϕ [$\text{B2}-\text{N}(5)-\text{Co}-\text{N}^*$, where N^* is the midpoint between $\text{N}(1)$ and $\text{N}(2)$, Table 2]. In the five Me_3Bzm imine/oxime structures, the Me_3Bzm plane bisects the two five-membered rings of the chelate ($\phi \sim 90^\circ$) only in the $-\text{CH}_2\text{CF}_3$ derivative. The Me_3Bzm plane in **1** ($\phi = 57^\circ$) and **3** ($\phi = 60^\circ$) is oriented such that the bulkier part of the ligand nearly eclipses a $\text{Co}-\text{N}(\text{imine})$ bond. In contrast, the Me_3Bzm ligand nearly eclipses a $\text{Co}-\text{N}(\text{oxime})$ bond for the $\text{R} = \text{CH}_2\text{CH}_3$ ($\phi = 119^\circ$) and CH_3 ($\phi = 115^\circ$) complexes. Thus, the range of observed orientations for Me_3Bzm is $\pm \sim 30^\circ$ from the plane bisecting the two five-membered rings of the chelate.

(31) Yohannes, P. G.; Bresciani-Pahor, N.; Randaccio, L.; Zangrando, E.; Marzilli, L. G. *Inorg. Chem.* **1988**, *27*, 4738.

(32) Polson, S.; Cini, R.; Marzilli, L. G. Manuscript in preparation.

(33) Randaccio, L.; Bresciani-Pahor, N.; Zangrando, E.; Marzilli, L. G. *Chem. Soc. Rev.* **1989**, *18*, 225.

(34) Calligaris, M. *J. Chem. Soc., Dalton Trans.* **1974**, 1628.

(35) Brückner, S.; Calligaris, M.; Nardin, G.; Randaccio, L. *Inorg. Chim. Acta* **1969**, *3*, 278.

(36) Marzilli, L. G.; Summers, M. F.; Bresciani-Pahor, N.; Zangrando, E.; Charland, J.-P.; Randaccio, L. *J. Am. Chem. Soc.* **1985**, *107*, 6880.

(37) Bresciani-Pahor, N.; Randaccio, L.; Zangrando, E. *Inorg. Chim. Acta* **1990**, *168*, 115.

(38) Parker, W. O., Jr.; Bresciani-Pahor, N.; Zangrando, E.; Randaccio, L.; Marzilli, L. G. *Inorg. Chem.* **1986**, *25*, 1303.

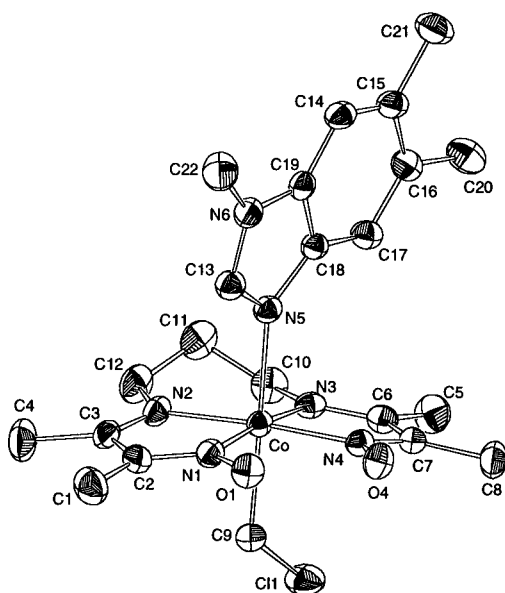


Figure 3. Perspective drawing of the complex molecule of **3** with the atom labels. Ellipsoids enclose 30% probability.

Table 2. Comparison of Geometric Parameters for [LCo((DO)(DOH)pn)R]PF₆ (L = Me₃Bzm, py) and Relevant LCo(DH)₂R Complexes Esd's: <0.007 Å for Co–C and Co–N(5) Distances; <0.001 Å for *d*; and <1° for the Angles ϕ , γ , and α

	Co–C, Å	Co–N(5), Å	ϕ , deg	γ , deg	α , deg	<i>d</i> , Å
[Me ₃ BzmCo((DO)(DOH)pn)R]PF ₆						
CH ₂ CF ₃ ^a	2.026(4)	2.060(3)	80	84	17	0.06
CH ₂ Cl	2.020(4)	2.088(3)	60	82	17	0.08
CH ₃ ^a	2.011(3)	2.100(3)	115	88	14	0.09
CH ₂ CH ₃ ^a	2.041(4)	2.105(5)	119	89	17	0.10
CH ₂ OCH ₃	2.065(5)	2.133(4)	57	83	15	0.08
Me ₃ BzmCo(DH) ₂ R						
CH ₃ ^b	1.989(2)	2.060(2)	14	89	5	0.06
CH ₂ CH ₃ ^c	2.027(7)	2.084(5)	0	89	4	0.05
CH ₂ OCH ₃ ^d	2.033(3)	2.093(2)	4	88	3	0.05
[pyCo((DO)(DOH)pn)R]PF ₆						
Cl ^{e,f}		1.993(6)	86	89	13	0.06
CH ₃ ^{f,g}	2.003(3)	2.106(3)	84	90	7	0.07
CH ₂ OCH ₃	2.028(3)	2.125(4)	88	78	15	0.07
<i>neo</i> -C ₅ H ₁₁ ^g	2.083(4)	2.121(3)	74	85	14	0.03
pyCo(DH) ₂ R						
Cl ^h		1.959(2)	6	89	2	0.00
CH ₃ ⁱ	1.998(5)	2.068(3)	1	89	3	0.05
<i>neo</i> -C ₅ H ₁₁ ^j	2.060(6)	2.081(4)	2	86	–5	0.00

^a Reference 17. ^b Reference 8. ^c Reference 39. ^d Unpublished results.

^e Reference 14. ^f C6 on R side of equatorial plane. ^g Reference 6.

^h Reference 40. ⁱ Reference 49. ^j Reference 41.

In **1** and **3**, there is a slight tilt of Me₃Bzm away from the 1,3-propanediyl bridge; γ , the angle between the L plane and the equatorial plane, is 83 and 82°, respectively. These tilt angles are similar to those for [Me₃BzmCo((DO)(DOH)-Me₂pn)CH₃]PF₆ ($\gamma = 81^\circ$)³¹ and [Me₃BzmCo((DO)(DOH)pn)-CH₂CF₃]PF₆ ($\gamma = 84^\circ$, calculated here). In two complexes (R = CH₃, CH₂CH₃; Table 2),^{6,8,14,17,39–41} Me₃Bzm does not tilt. In two of the four known X-ray crystal structures of [pyCo((DO)(DOH)pn)R]PF₆ compounds, py is tilted in the R = *neo*-C₅H₁₁ and CH₂OCH₃ (**2**) structures (Table 2). The tilting of L

is unlikely to be a consequence of the orientation of the central CH₂ of the 1,3-propanediyl bridge with respect to the L plane, since the CH₂ group and L plane are well separated. In addition, we expect that steric interference by the propylene bridge would cause tilting of the Co–N bond with the L plane (i.e., distortion of the C–Co–N bond angle). Tilting is most likely to be just a result of the crystal packing forces.

For [Me₃BzmCo((DO)(DOH)pn)R]PF₆ compounds, the chemically equivalent halves in the equatorial ligand are bent away from L (the dihedral angle, α , between the chemically equivalent halves in the equatorial ligand, Table 2). There is no trend in the α values: lower α values are expected for bulkier ligands, but the value is smallest for CH₃. The Co atom is displaced from the least-squares plane of the equatorial donors by 0.06–0.10 Å toward the axial N(5) donor. The Co–N(5) bond lengths for **1** and **3** are 2.133(4) and 2.088(3) Å, respectively. The trend of increasing Co–N(5) bond length for Me₃Bzm imine/oxime complexes with increasing electron-donating ability of the R group agrees with that found in cobaloximes⁵ (Table 2): CH₂CF₃ < CH₂Cl < CH₃ < CH₂CH₃ < CH₂OCH₃. This trend illustrates the strong *trans* influence of the –CH₂OCH₃ group, similar to that of *neo*-C₅H₁₁ (Table 2).¹⁷

In the crystal structure for [pyCo((DO)(DOH)pn)CH₂OCH₃]PF₆ (**2**, Table 2), the ϕ angle ($\phi = 88^\circ$) is normal for [pyCo((DO)(DOH)pn)R]PF₆ complexes.⁶ The trend in the α values of the py complexes also does not correlate with the relative bulk of the R or X group; the –CH₃ complex has an unusually low α value. The Co–N(5) bond length of **2** is similar to that of the R = *neo*-C₅H₁₁ complex, as expected.

Although for the [LCo((DO)(DOH)pn)CH₂OCH₃]PF₆ compounds, the Co–C bond distance in **1** (2.065(5) Å, L = Me₃Bzm) is longer than that in **2** (2.028(3) Å, L = py) by ~7 times the esd (just statistically significant), there is no significant difference in the Co–C bond lengths for the analogous Co–CH₃ complexes (Table 2). For a given R, regardless of bulk, the Co–C bond lengths are similar for the py and the Me₃Bzm cobaloximes (Supporting Information).

The Co–N(5) bond distances for **1** and **2** are very similar. This is expected since, despite the larger C–N(5)–C angle of py vs Me₃Bzm, Me₃Bzm is lopsided with a bulky benzene ring. Thus, the effective steric size of the two ligands around the metal is similar.¹⁷ Values of the Co–N(5) bond distance (L = Me₃Bzm, py) for cobaloximes have a good linear relationship ($r^2 =$ correlation of determination⁴² = 0.979, slope = 1.00) with the Co–N(5) distances for the corresponding imine/oxime complex ($n =$ number of compounds = 6). The Co–N(5) bond lengths for imine/oxime compounds (L = py, Me₃Bzm) were found to be ~0.03 Å longer than those for the cobaloxime analogs.

The orientations of the –CH₂OCH₃ group around the Co–C bonds are different in **1** and **2**. The N*–Co–C–O dihedral angles are 63.3(3)° for **1** (nearly eclipses a Co–N(oxime) bond) and 176.7(3)° for **2**. The orientation of the C–O bond over the central methylene group, C(6), in **2** is unusual, since the C–X bond of the alkyl group typically is aligned with a Co–N bond for both imine/oxime-type and cobaloxime B₁₂ models.¹⁷ The likely cause of this deviation from the trend of C–X axial bond alignment is crystal packing forces.

The imine/oxime complexes and the cobaloxime complexes appear to exhibit the same relationships between electron-donating ability and key bond lengths. The longer Co–N(5) bonds of the imine/oxime-type complexes compared to the corresponding cobaloximes make them better structural models

(39) Solans, X.; Gómez, M.; López, C. *Transition Met. Chem.* **1991**, *16*, 176.

(40) Geremia, S.; Dreos, R.; Randaccio, L.; Tazher, G.; Antolini, L. *Inorg. Chim. Acta* **1994**, *216*, 125.

(41) Randaccio, L.; Bresciani-Pahor, N.; Toscano, P. J.; Marzilli, L. G. *J. Am. Chem. Soc.* **1981**, *103*, 6347.

(42) Daniel, W. W. *Biostatistics: A Foundation for Analysis in the Health Sciences*, 5th ed.; Wiley & Sons: New York, 1991.

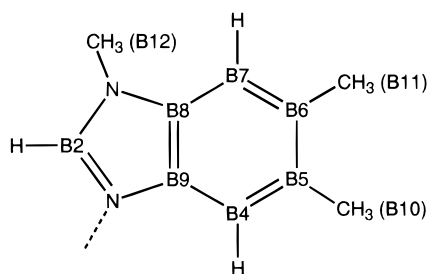


Figure 4. Atom-labeling scheme for Me₃Bzm.

for the B₁₂ coenzymes. For L = Me₃Bzm, the Co–C bonds for the imine/oxime-type complexes are slightly longer (0.01–0.03 Å) than for cobaloximes (Table 2, Supporting Information). Although it is slight, a dependence of Co–C bond length on the equatorial ligand has not been noted previously. However, for both B₁₂ model systems these distances are comparable to the known Co–C bond distances of the B₁₂ cofactors (1.99–2.03 Å).¹⁷

NMR Studies. The ¹³C NMR results on the newly extended series of imine/oxime-type complexes can be compared quantitatively with the electronic parameter (EP)⁴ and with ¹³C NMR results for the cobaloximes.^{4,7,43,44} EP, a measure of the electronic *trans* influence, is derived primarily from ¹³C NMR data for pyCo(DH)₂R(or X) compounds.⁴ However, in general, EP also reflects the structural *trans* influence.

¹³C NMR. Me₃Bzm Complexes. ¹³C and ¹H NMR signal assignments for Me₃Bzm refer to the atom-labeling scheme given in Figure 4. Table 3 and the Supporting Information give ¹³C NMR data for [Me₃BzmCo((DO)(DOH)pn)R]⁺ salts in CDCl₃ (ClO₄) and DMSO-*d*₆ (PF₆), respectively. We had previously assigned¹⁷ B5, B6, and B8 shifts by comparison to data in earlier reports,^{44–46} and we used the same logic to assign the ¹³C NMR signals for the new compounds. Correlations of ¹³C NMR data for imine/oximes with those for cobaloximes (see below) facilitated the assignment of the ¹³C NMR shifts of [Me₃BzmCo((DO)(DOH)pn)Cl]ClO₄.

For [Me₃BzmCo((DO)(DOH)pn)R(or X)]ClO₄ in CDCl₃ (*n* = 11; EP range –1.56 for X = Cl to +0.24 for R = CH₂OCH₃), we found that the B5, B6, B9, B12, oxime C, imine C, and oxime CH₃ shifts correlated very well with EP (Table 4, *r*² > 0.90), and the B4, B7, and imine CH₃ shifts exhibited strong correlations (*r*² > 0.80). These signals correlated reasonably well with corresponding Me₃Bzm shifts in the related cobaloximes (*r*² > 0.80; *n* = 10; EP range –1.56 to +0.24; Figure 5, Table 4). However, the correlation with EP was better for the cobaloximes than for the imine/oxime complexes (Table 4). While the cobaloxime B8 shift correlated with EP, it did not correlate with the corresponding imine/oxime B8 shift (Figure 6, Table 4), which displayed no apparent trend with EP.

The DMSO-*d*₆ data set was limited to *n* = 10, since the chloro complex exhibited complicated ligand-exchange behavior in this solvent. The ¹³C NMR shift data in DMSO-*d*₆ correlated better with EP (Table 4) than the data for the same 10 complexes in CDCl₃.

The above correlations of ¹³C NMR shifts for [Me₃BzmCo((DO)(DOH)pn)R(or X)]⁺ (in CDCl₃ and DMSO-*d*₆) with EP allowed us to determine an EP value for –CH₂SCH₃. The equation for each good linear fit and the appropriate ¹³C NMR

shift for the R = CH₂SCH₃ complex were used to calculate an EP value. The resulting EP values were averaged to give EP = –0.06 for –CH₂SCH₃. This value is similar to the EP value (–0.02) of [pyCo((DO)(DOH)pn)CH₂SCH₃]ClO₄ (generated *in situ* in CDCl₃) calculated from the γ -C shift by the method used for cobaloximes.⁴ Thus, –CH₂SCH₃ exerts a *trans* influence similar to that of –CH₃ (EP = 0).

¹H NMR. Me₃Bzm Complexes. Our assignments for [Me₃BzmCo((DO)(DOH)pn)R]⁺ salts in CDCl₃ (Table 5 (ClO₄), Supporting Information (PF₆)) agree with previous assignments¹⁷ that the most downfield signal is H2. However, we assigned the least variable signal (δ 7.13–7.16 ppm) to H7, on the basis of remoteness of H7 from Co and the free Me₃Bzm value of 7.15 ppm. Only for the low EP ligands, Cl and N₃, does the H7 signal (7.10 ppm) lie outside this range. The H4 signal (range δ 7.02–7.36 ppm for perchlorate salts) was either upfield or downfield of the H7 signal. We observed sharp signals in the spectrum for [Me₃BzmCo((DO)(DOH)pn)CH₂OCH₃]PF₆; however, the spectrum of the perchlorate salt displayed broad signals. We suspect that trace Co^{II} species are present.

In contrast to the earlier observations on fewer compounds,¹⁷ we found that the H2 shift of the Me₃Bzm adducts did not appear to be of a similar value for complexes with axial groups of similar electron-donating abilities. For example, spectra of the R = CH₂NO₂ and CH₂CH₃ compounds exhibited the same H2 shifts (Table 5). The most upfield H2 shift occurred for the R = *neo*-C₅H₁₁ complex (0.22 ppm upfield of R = CH₃ in CDCl₃, Table 5).

Aqua and Py Complexes. ¹H NMR signals for [H₂OCo((DO)(DOH)pn)R]ClO₄(or PF₆) in DMSO-*d*₆ (Supporting Information) were assigned on the basis of earlier assignments¹⁷ for compounds of this type. Our ¹H NMR assignments for [pyCo((DO)(DOH)pn)R]ClO₄ complexes in CDCl₃ (Supporting Information) were based on those for [pyCo((DO)(DOH)pn)CH₃]ClO₄, which were made using 1D NOE techniques.¹⁷ The poor solubility of the py derivatives of negative axial ligands with low EP values makes drawing any conclusions difficult. In general, the shifts for the R = CH₂OCH₃ derivative are consistent with a high *trans* influence for this alkyl group.

Correlation of NMR and Structural Properties. Numerous studies, particularly with cobaloximes,^{4,5,7,11,43} show a relationship between structure and NMR chemical shift. In addition to ¹³C NMR shifts, Co–N(5) bond lengths are another measure of *trans* influence. Thus, we compared the ¹³C NMR shifts for [Me₃BzmCo((DO)(DOH)pn)R(or X)]ClO₄ in CDCl₃ with the corresponding Co–N(5) length (*n* = 5). We found that the best correlations of Co–N bond length were with the B5, B6, B9, B12, imine CH₃, and oxime CH₃ signals (*r*² > 0.80, Supporting Information). Since the imine C and oxime C ¹³C NMR shifts did not show a strong correlation with Co–N(5) bond length, these shifts are not a good indicator of the structural *trans* influence.

Interestingly, the Co–N(5) bond lengths for the five structurally characterized Me₃Bzm imine/oxime complexes (Table 2) correlated better with cobaloxime B4, B5, B6, B7, and B8 shifts than with the corresponding imine/oxime shifts (Supporting Information). The better correlation found and the other differences in behavior of shifts for the two model systems, as noted above, probably have a structural basis. In particular, the two models differ in the orientation of the planar Me₃Bzm ligand with respect to the equatorial plane (Figure 7). For cobaloximes, the planar Me₃Bzm ligand has orientation A. In cobaloximes, the *trans* R or X ligand bulk will lead to distortion

(43) Brown, K. L.; Satyanarayana, S. *J. Am. Chem. Soc.* **1992**, *114*, 5674.

(44) Brown, K. L.; Hakimi, J. M. *J. Am. Chem. Soc.* **1986**, *108*, 496.

(45) Brown, K. L.; Hakimi, J. M.; Nuss, D. M.; Montejano, Y. D. *Inorg. Chem.* **1984**, *23*, 1463.

(46) Summers, M. F.; Marzilli, L. G.; Bax, A. *J. Am. Chem. Soc.* **1986**, *108*, 4285.

Table 3. ¹³C NMR Chemical Shifts (ppm) of Me₃Bzm and [Me₃BzmCo((DO)(DOH)pn)R(or X)]ClO₄ Complexes in CDCl₃ in Order of EP Value

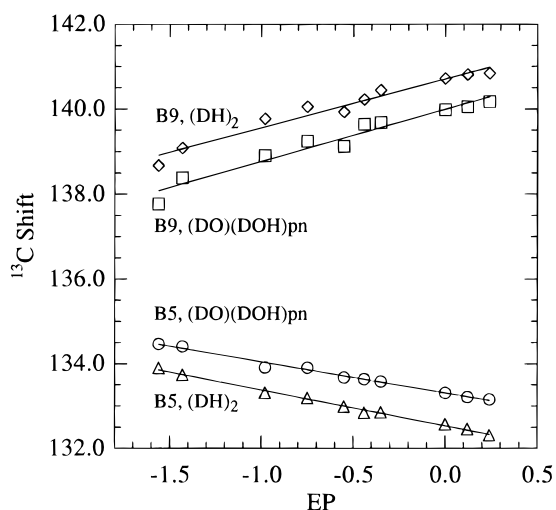
	B2	B4	B5	B6	B7	B8	B9	B10	B11	B12	imine C	oxime C	NCH ₂ CH ₂ CH ₂ N	NCH ₂ CH ₂ CH ₂ N	imine CH ₃	oxime CH ₃
Cl	143.87	116.17	134.47	133.76	111.41	132.93	137.77	20.82	20.20	32.44	177.89	157.46	49.90	27.50	18.58	13.98
N ₃	144.51	116.35	134.41	133.68	111.32	133.11	138.38	20.88	20.24	32.42	177.09	156.43	49.86	27.48	18.50	13.82
CH ₂ NO ₂	144.38	116.26	133.92	133.08	111.40	133.53	138.90	20.88	20.23	32.20	176.72	156.27	48.79	27.12	18.54	13.54
CH ₂ CN	144.13	116.70	133.91	133.10	111.06	133.22	139.24	20.74	20.30	32.09	175.81	155.70	49.13	27.60	18.59	13.38
CH ₂ CF ₃	144.06	116.53	133.68	132.80	111.17	133.51	139.12	20.79	20.24	32.05	175.75	155.47	49.18	27.20	17.89	13.15
CH ₂ CO ₂ CH ₃	144.31	116.55	133.58	132.69	111.16	133.58	139.29	20.82	20.24	32.07	175.26	155.23	48.98	27.10	18.00	13.27
CH ₂ Br	144.51	116.98	133.64	132.80	110.92	133.34	139.64	20.74	20.28	32.03	174.42	154.73	49.18	27.18	17.99	13.14
CH ₂ Cl	144.42	116.96	133.58	132.73	110.94	133.39	139.68	20.74	20.27	31.97	174.33	154.70	49.29	27.24	17.80	13.05
CH ₂ SCH ₃	144.68	117.01	133.32	132.05	110.93	133.66	a	20.80	20.32	31.97	173.59	154.11	49.10	27.40	17.82	13.12
CH ₃	144.28	117.10	133.31	132.41	110.78	133.50	139.98	20.71	20.30	31.89	172.57	153.30	49.37	27.41	17.44	12.89
CH ₂ CH ₃	144.26	117.12	133.21	132.28	110.81	133.61	140.05	20.73	20.28	31.85	172.71	153.42	49.13	27.17	17.44	12.88
CH ₂ OCH ₃ ^b	144.37	117.02	133.16	132.16	110.85	133.11	140.17	20.73	20.27	31.84	172.87	153.79	49.19	27.33	17.32	12.81
Me ₃ Bzm ^c	142.80	120.29	132.05	130.84	109.51	133.21	142.50	20.53	20.20	30.87						

^a Data not observed. ^b Exchange of Me₃Bzm observed; B5, B6 signals very close in shift. ^c Reference 17.

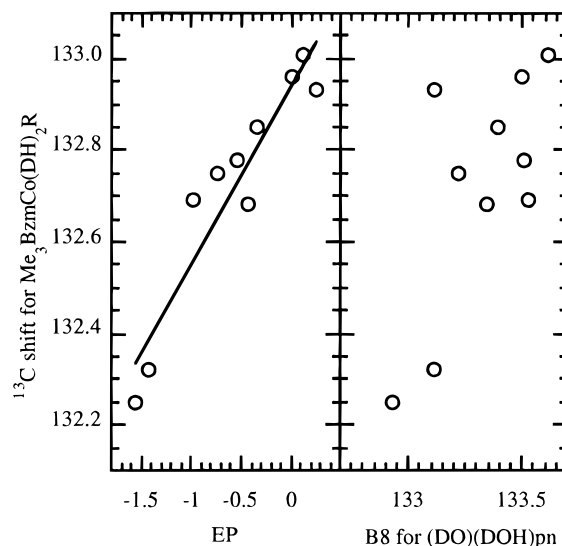
Table 4. Correlation (r^2) of ¹³C NMR Shift Data for the [Me₃BzmCo((DO)(DOH)pn)R]ClO₄ Series (in CDCl₃ and DMSO-*d*₆) with EP and with Relevant Cobaloximes and Correlation of ¹³C NMR Shift Data for Me₃BzmCo(DH)₂R (in CDCl₃) with EP

solvent	(DO)(DOH)pn ^a		(DH) ₂ vs (DO)(DOH)pn ^d	
	CDCl ₃	DMSO- <i>d</i> ₆	CDCl ₃	CDCl ₃
B2	0.073	0.282	0.750	0.183
B4	0.814	0.838	0.973	0.847
B5	0.986	0.979	0.995	0.991
B6	0.980	0.995	0.993	0.986
B7	0.828	0.947	0.974	0.811
B8	0.256	0.302	0.893	0.488
B9	0.949	0.951	0.958	0.988
B12	0.979	0.986	0.988	0.985
imine C	0.937	0.956		
oxime C	0.928	0.951		
imine CH ₃	0.851	0.914		
oxime CH ₃	0.977	0.984		

^a $n = 11$. ^b $n = 10$; R = Cl complex excluded. ^c Reference 17. ^d $n = 10$; R = CH₂CO₂CH₃ not available.

**Figure 5.** Plots of B5 and B9 ¹³C NMR shifts (ppm) vs EP for [Me₃BzmCo(CHEL)R(or X)]⁰⁺. CHEL = (DH)₂, (DO)(DOH)pn.

of the (DH)₂ group from planarity on either side of the axis passing through the oxime H atoms. Such a distortion will have a minimum steric effect on the Me₃Bzm ligand. In contrast, in imine/oxime compounds the Me₃Bzm ligand has orientation B. In this orientation the steric interaction with the equatorial imine/oxime ligand is probably responsible for the longer Co–N(5) bonds in these complexes. Any dependence of the steric effect on the shape and size of the negative axial ligand could then modify the structure of the bound Me₃Bzm slightly, leading to

**Figure 6.** Plots of the B8 ¹³C NMR shift (ppm) for Me₃BzmCo(DH)₂R (or X) vs EP (left) and vs the B8 ¹³C NMR shift for [Me₃BzmCo((DO)(DOH)pn)R(or X)]ClO₄ (right); $n = 10$.

small effects on ¹³C shifts. Since such effects are not directly related to the electronic changes in R or X, correlations with EP and with shifts of other (nonsterically sensitive) carbons are poor.

We believe that B8, which is at the juncture of the two rings of Me₃Bzm, may be particularly susceptible to this steric effect. The erratic shift dependence of the signal of this carbon could thereby be rationalized. This dependence on steric effect leads to B8 having a poor correlation for imine/oxime compounds (and a significantly lower one in cobaloximes), Table 4. Other signals that may reflect this steric effect for the imine/oxime complexes, but to a lower degree, are B4 and B7. It is not clear why B2 exhibits such poor correlations, but this signal has a relatively small shift range, and any effect of the anisotropy of Co and of the equatorial ligand may make a relatively large contribution compared to the equivalent carbon on the other side of the ligating N, namely B9. Even from the earliest ¹³C NMR study of a B₁₂ model,⁴⁷ it was clear that signals for carbons close to the metal center exhibit anomalous behavior. We can now suggest that the signals that provide the most reliable measure of the electronic properties of the Co center are those for carbons that are *both* well removed from the Co and not susceptible to steric strain.

Table 5. ^1H NMR Shifts (ppm) of Me_3Bzm and $[\text{Me}_3\text{BzmCo}(\text{DO})(\text{DOH})\text{pnR}(\text{or X})]\text{ClO}_4$ Complexes in CDCl_3

	EP	H2	H4	H7	B11H3	B10H3	OH...O	NCH ₂ CCH ₂ N		imine CH ₃	oxime CH ₃	NCH ₃
Cl	-1.56	7.53	7.36	7.10	2.35	2.32	19.14	4.44	4.18	2.67	2.55	3.89
N ₃	-1.43	7.69	7.24	7.10	2.35	2.34	18.91	4.38	4.03	2.71	2.58	3.92
CH ₂ NO ₂	-0.98	7.58	7.02	7.16	2.33	2.32	18.66	4.14	3.84	2.59	2.45	3.90
CH ₂ CN	-0.75	7.65	7.32	7.16	2.36	2.35	18.99	4.15	3.99	2.54	2.37	3.91
CH ₂ CF ₃	-0.55	7.56	7.11	7.16	2.33	2.32	18.90	4.17	3.78	2.50	2.36	3.89
CH ₂ CO ₂ CH ₃	-0.49	7.56	7.05	7.14	2.33	2.31	18.85	4.15	3.75	2.53	2.41	3.89
CH ₂ Br	-0.44	7.73	7.28	7.16	2.34	2.33	18.90	4.12	3.83	2.47	2.33	3.93
CH ₂ Cl	-0.35	7.68	7.23	7.16	2.34	2.32	18.92	4.08	3.82	2.46	2.32	3.91
CH ₂ SCH ₃	-0.06	7.63	7.09	7.15	2.34	2.31	19.06	4.07	3.63	2.48	2.37	3.90
CH ₃	0	7.66	7.26	7.15	2.34	2.32	19.22	4.10	3.79	2.41	2.29	3.91
CH ₂ CH ₃	0.12	7.58	7.12	7.15	2.33	2.31	19.10	4.08	3.70	2.43	2.31	3.89
<i>neo</i> -C ₅ H ₁₁ ^a	0.19	7.44	7.03	7.13 ^a	2.34	2.31	19.40	4.19	3.66	2.45	2.30	3.87
CH ₂ OCH ₃ ^b	0.24	7.55	7.04	7.15	2.34	2.31	19.19	4.06	3.64	2.41	2.31	3.90
Me ₃ Bzm		7.74	7.55	7.15	2.40	2.38						

^a H4 and H7 assignments switched from literature values. ^b Broad aromatic signals.

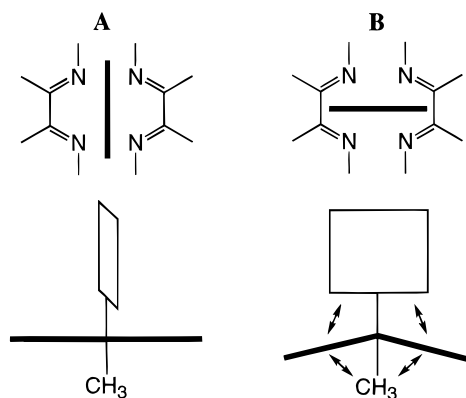


Figure 7. Schematic representation of the relationship of planar N-ligand orientation to butterfly bending.

Conclusions

The expanded series of well-defined Me_3Bzm imine/oxime type B_{12} models has provided important insight into the previously poorly understood phenomenon that ^{13}C NMR shifts of some carbons correlated well between models and the natural compounds whereas others did not. This lack of correlation can be attributed to differences in axial-ligand to equatorial-ligand steric strain between the various systems, not to different binding interactions across the different classes. When all the steric factors are taken into account, the relationships of ligand-dependent trends in model systems to those in B_{12} cofactors now appear to be more firmly established.

It is clear from the properties of the newly available imine/oxime complexes that these are not less stable nor more likely to undergo decomposition than the cobaloximes. In fact, we were able to prepare imine/oxime complexes with $\text{R} = \text{CH}_2\text{SCH}_3$. Cobaloximes with this alkyl group are not known. The more limited number of compounds available for the imine/oxime type of B_{12} models is mainly attributable to complications associated with synthetic routes. Careful selection of reaction conditions, routes, or the neutral axial ligand can allow the synthesis of complexes with new negative axial ligands. For example, we found that if L is *N*-MeImd, a good donor, the

chloro complex can be converted to the $-\text{CH}_2\text{NO}_2$ complex even with the harsh conditions needed for the conversion. Likewise, problems in preparing imine/oxime complexes of $-\text{CH}_2\text{OCH}_3$ by the $-\text{CH}_2\text{Br} + \text{methoxide}$ route can be overcome by using the $\text{Co}^1(\text{CO}) + \text{CH}_3\text{OCH}_2\text{Br}$ method.

The imine/oxime complexes exhibited the same relationships between electron-donating ability and key bond lengths as the cobaloxime complexes. The new results allowed us to note the slightly longer Co–C bonds (0.01–0.03 Å for $\text{L} = \text{Me}_3\text{Bzm}$) and longer Co–N(5) bonds (0.03 Å) of the imine/oxime-type complexes compared to cobaloximes, which indicate a slight dependence of Co–C and Co–N(5) bond lengths on the equatorial ligand. These dependencies are attributable to steric effects between the axial and the equatorial ligands. Recent FT-Raman data of solutions suggest that the sterically induced bond lengthening apparent in the solids undoubtedly also occurs in solution.⁴⁸ We found a tilt of the neutral ligand L with respect to the equatorial plane toward the O–H...O bridge in some imine/oxime compounds. The absence of a correlation between the tilt of L and molecular features such as the bulk of R suggests that the tilt results from intermolecular forces in the crystal.

Acknowledgment. This work was supported by NIH Grant GM 29225 (to L.G.M.). Instrument purchases were funded by the NIH and NSF. NSF Grant ASC-9527186 supported our use of the Internet for remote collaborative research.

Supporting Information Available: Tables of elemental analyses, additional NMR data, and correlations of NMR and structural data, packing diagrams and tables of crystallographic data for **1–3**, including X-ray experimental details, atomic coordinates, displacement parameters, thermal parameters, bond distances, and bond angles, and text presenting further details of the solution and refinement of the structures and additional structural comparisons (30 pages). Ordering information is given on any current masthead page.

IC961105Z

(48) Hirota, S.; Polson, S. M.; Puckett, J. M., Jr.; Moore, S. J.; Mitchell, M. B.; Marzilli, L. G. *Inorg. Chem.* **1996**, *35*, 5646.

(49) Bigotto, A.; Zangrando, E.; Randaccio, L. *J. Chem. Soc., Dalton Trans.* **1976**, 96.